

# *Recovery and recrystallization of electrodeposited bright copper coatings at room temperature. II. X-ray investigation of primary recrystallization*

I. V. TOMOV, D. S. STOYCHEV, I. B. VITANOVA

*Institute of Physical Chemistry, Bulgarian Academy of Sciences, 1040 Sofia, Bulgaria*

Received 5 March 1984; revised 3 October 1984

X-ray investigations of the recrystallization processes occurring at room temperature in electrodeposited bright copper coatings were carried out *in situ*. As a result of the orientation transformation of the growth texture with  $\langle 311 \rangle$ ,  $\langle 111 \rangle$  and  $\langle 110 \rangle$  components, a recrystallization texture with  $\langle 100 \rangle$ ,  $\langle 110 \rangle$  and  $\langle 111 \rangle$  components was obtained. It was established that one of the factors which influence the microhardness of copper coatings is the orientation distribution of crystallites.

## 1. Introduction

Generally, primary recrystallization is initiated by thermal activation [1, 2]. However, Cook and Richards have observed recovery and recrystallization of pure, highly conductive copper at room temperature [3]. Recrystallization at room temperature has also been found for copper and other metals by Megaw and Stokes [4].

Recrystallization of metallic materials is always accompanied by a change in their physical and mechanical properties [1-4]. In many cases, however, it has been found that an orientation relationship exists between the new grains and the grains of the deformed matrix from which they grow [1-3, 5-14].

The aim of the present paper is to investigate the orientation transformations between the growth texture produced during the electrodeposition of copper coatings and its resultant recrystallization texture. An attempt is made to estimate the effect of recrystallization on the microhardness of electrodeposited copper coatings.

## 2. Expressing volume fractions of texture components in ideal directions

For the qualitative as well as for the quantitative estimation of the textures it is necessary to measure experimentally their pole figures. In the

case of a multicomponent texture, the different texture components  $\langle hkl \rangle$  can be quantitatively estimated by the volume fractions  $M_{hkl}$ . If the textures are sharp,  $M_{hkl}$  can be determined using the method developed by Tomov and Bunge [15]. This method is not convenient, however, for characterizing 'smeared out' fibre textures. In this case it is appropriate to use the method of Harris [16], which allows the inverse pole figure to be calculated. The value  $R_{hkl}$  of the inverse pole figure in the  $hkl$  direction is expressed by the equation

$$R_{hkl} = \frac{I_{hkl}}{(I_{hkl})_r} \bigg/ \frac{1}{n} \sum_{hkl} \frac{I_{hkl}}{(I_{hkl})_r} \quad (1)$$

where  $I_{hkl}$  is the experimentally measured intensity of the reflections,  $\langle hkl \rangle$ , of the textured sample;  $n$  is the total number of reflections measured;  $(I_{hkl})_r$  is the reflection intensity of a random sample of the same material.

If the assumption is made that only crystallites with orientations in the experimentally measured directions occur, then the volume fractions  $M_{hkl}$  of the respective components can be expressed by the values  $R_{hkl}$ :

$$M_{hkl} = \frac{R_{hkl}}{\sum_{hkl} R_{hkl}} \quad (2)$$

### 3. Sample preparation

The conditions of bright copper coating electro-deposition have already been described in [17]. These coatings represent fibre textures. The present work examined the recrystallization of samples with rapidly (number 162) and slowly (number 163) falling microhardness.

### 4. Experimental technique

Pole figures  $P_{hkl}(\phi)$  were measured by using a texture goniometer in the reflection mode with  $\text{CoK}\alpha$ -radiation. The intensities  $I_{hkl}$  were measured by means of an X-ray diffractometer with  $\text{CoK}\beta$ -radiation monochromatized with a curved crystal monochromator.\*

The establishing of the initial moment of recrystallization as well as the visual control of the continuing process were carried out using a small Debye-Scherrer camera with an asymmetrically located film. The sample studied was  $8 \times 8$  mm and  $140 \mu\text{m}$  thick. The diagram of the experiment in the Debye-Scherrer camera (diagram of back reflection) is presented in Fig. 1. The direction of the initial beam SO coincides with the fibre axis F (normal to the copper coating surface). The normal N to the reflecting planes  $\{100\}$  divides the diffraction angle ( $180 - 2\theta$ ) in half. The angle  $\phi$  (SON) is formed

by the fibre axis F and the normal N. The connection between Bragg angle  $\theta$  and angle  $\phi$  can easily be found from the equation

$$\phi = 90^\circ - \theta \quad (3)$$

$\text{CoK}\alpha$ -radiation monochromatized with a flat crystal monochromator was employed. The exposure lasted 3 h. The photographic film was changed daily in the course of the investigation, with due care taken to avoid disturbing the copper sample. Thus the study of one and the same sample volume was ensured during the entire process of recrystallization.

Samples  $35 \times 35$  mm and  $140 \mu\text{m}$  thick were measured with a texture goniometer and X-ray diffractometer.

### 5. Experimental results and discussion

#### 5.1. Identification of recrystallization texture component $\langle 100 \rangle$

The initiation of recrystallization texture and, in particular, the  $\langle 100 \rangle$  component becomes evident from the investigations performed by X-ray photographic registration. By using the scheme in Fig. 1 for taking X-ray pictures, Debye rings 400, 222 and 311 can be registered (Fig. 2). The crystallites, whose  $\langle 100 \rangle$  planes join at an angle of  $\theta = 82.2^\circ$ , reflect the Debye ring 400 (Fig. 1). Their crystallographic axes  $\langle 100 \rangle$  are parallel to the normal N and according to Equation 3 they join with the fibre axis F at an angle of  $\phi = 7.8^\circ$ . Therefore these crystallites belong to the  $\langle 100 \rangle$  texture component regardless of the fact that their  $\langle 100 \rangle$  axes divert  $7.8^\circ$  from the ideal position of the  $\langle 100 \rangle$  component. The Debye ring 400 of sample number 162, registered on the first day after electrodeposition, is strongly diffused (Fig. 2a). It is located at a Bragg angle of  $\theta = 82.2^\circ$ , where the microdeformation contribution to its broadening is rather considerable. At equal microdeformations the ring 400 would be about 4.5 times more diffused in the radial direction than its neighbouring ring 222.

When a sharp black spot appears on the diffuse ring 400, it is due to the recrystallization grain belonging to the  $\langle 100 \rangle$  texture component. The sharpness of the spot is due to the lattice perfection of the recrystallization grain. The number of

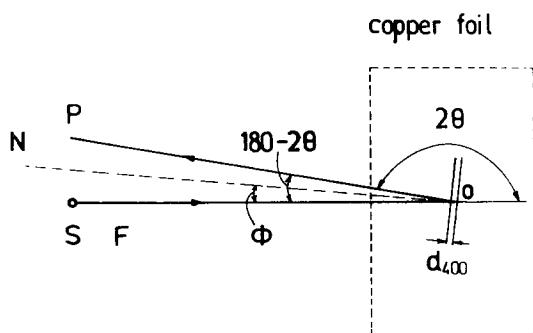


Fig. 1. Back reflection diagram in Debye-Scherrer camera. S, focus of X-ray tube; F, fibre axis; SO, initial X-ray beam; OP, diffracted X-ray beam;  $d_{400}$ , interplanary distance 400; N, normal to the reflecting planes;  $2\theta$ , diffraction angle;  $\phi$ , angle between the fibre axis and the normal to the reflecting plane.

\* The X-ray experiments for determining the microdeformations, apparent crystallite size (see [17]) and inverse pole figures were carried out simultaneously. In all cases  $\text{CoK}\beta$ -radiation was used.

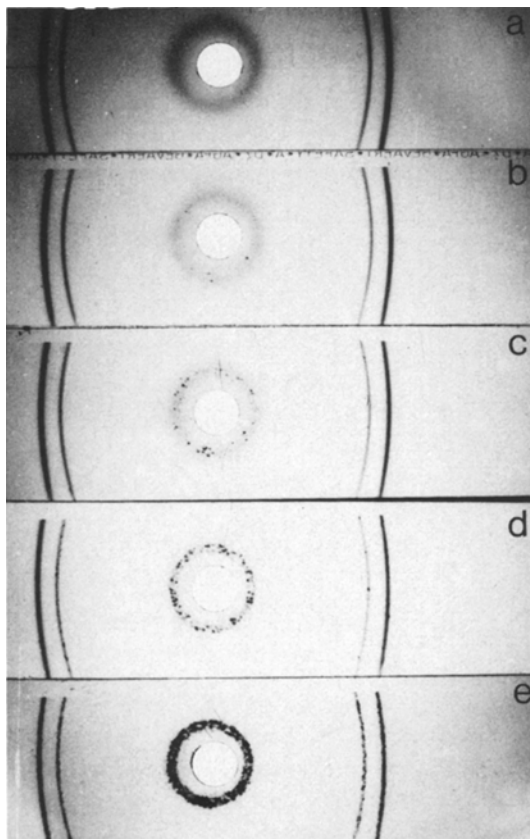


Fig. 2. X-ray pictures taken using the Debye-Scherrer camera with back reflection mode ( $\text{CoK}\alpha$ -radiation, flat crystal monochromator). Debye rings 311, 222 and 400 are registered. Diffuse ring 400 is due to strained crystal matrix. The sharp black spots are due to recrystallized crystallites.

recrystallization grains with  $\langle 100 \rangle$  orientation increases continuously, uniformly filling the whole 400 ring. Finally, it can be observed (Fig. 2e) that lines 222 and 311 also become spotty, indicating that the entire or the greater part of the deformed matrix is consumed by recrystallized grains.

During the entire period of recrystallization study in the Debye-Scherrer camera, the primary X-ray beam was incident on only one spot of the sample. Information about the recrystallization proceeding in the copper sample bulk was acquired by determining the spot size and the effective depth of X-ray penetration. The results recorded could in no way be influenced by ambient effects and can be due to grains situated both on the surface and in the bulk of the sample. Observed by means of an optical microscope,

etching can essentially change the consequent course of recrystallization, as indicated by Brucke and Turnbull [1]. In this sense the method used seems to be similar to electron microscopy; however being absolutely selective, it allows the observation only of the grains which have recrystallized. Another advantage is that the recrystallization process is studied *in situ*.

For sample number 162 the presence of recrystallized grains was established on the second day after electrodeposition (see Fig. 2b). On sample number 163 recrystallized grains were observed on the seventh day after electrodeposition. Moreover, their number, as compared to the number of grains in sample number 162, increased considerably more slowly with time.

### 5.2. Qualitative texture investigation

Qualitative information about the texture was obtained by measuring pole figures  $\{111\}$ ,  $\{100\}$ ,  $\{110\}$  and  $\{311\}$ . The pole figures given in Fig. 3 were measured on the first day after electrodeposition of sample number 163 when its microhardness was about 235 HV. The texture is smeared out, but the presence of components  $\langle 311 \rangle$ ,  $\langle 111 \rangle$  and to a lesser extent  $\langle 110 \rangle$ , is evident. After a certain period, at a sample microhardness of approximately 140 HV, three texture components, i.e.  $\langle 100 \rangle$ ,  $\langle 110 \rangle$  and  $\langle 111 \rangle$  are also observed. As a result of the orientation recrystallization, texture component  $\langle 311 \rangle$  has completely disappeared. Sample number 162, in the microhardness interval 240–140 HV, manifests texture and changes similar to sample number 163. On the pole figures  $P_{100}(\phi)$  (Figs 3, 4) are dotted the angle intervals within which the crystallites reflecting in Debye ring 400 contribute (Fig. 2). This affirmation follows from Equation 3. It is seen from the pole figure that these grains belong to the  $\langle 110 \rangle$  texture component. Abrupt transitions in the pole distribution in Figs 3 and 4 are due to separate crystallites becoming recrystallized to considerable sizes.

### 5.3. Dependence of microhardness on orientation distribution

From the pictures obtained with the Debye-

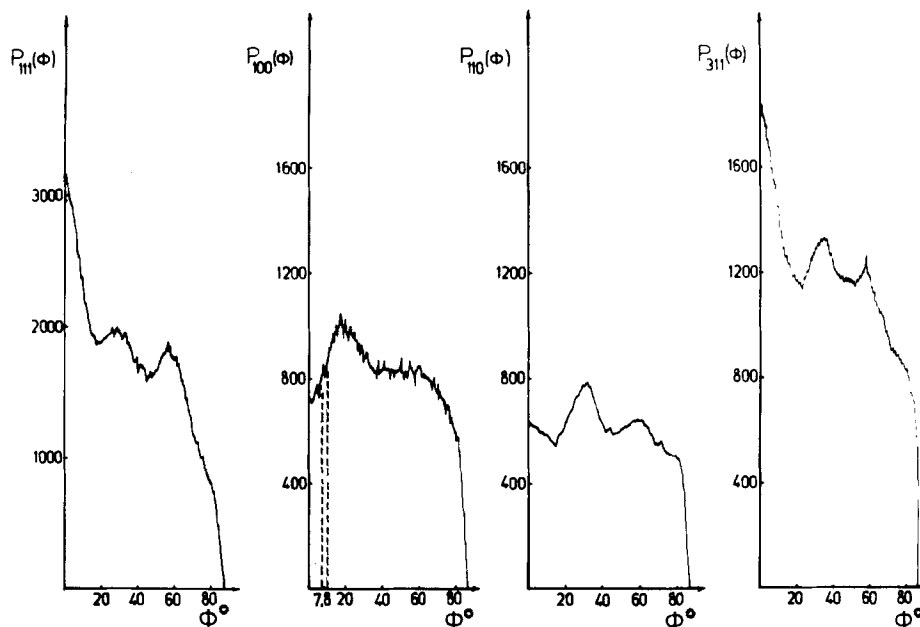


Fig. 3. Pole figures  $\{111\}$ ,  $\{100\}$ ,  $\{110\}$  and  $\{311\}$  of copper foils obtained by plating. Main texture components are  $\langle 311 \rangle$  and  $\langle 111 \rangle$ ; the  $\langle 110 \rangle$  component is also observed. The dotted line on angle  $\phi = 7.8^\circ$  marks the region where crystallites of component  $\langle 100 \rangle$  reflect, reflecting also the Debye ring 400.

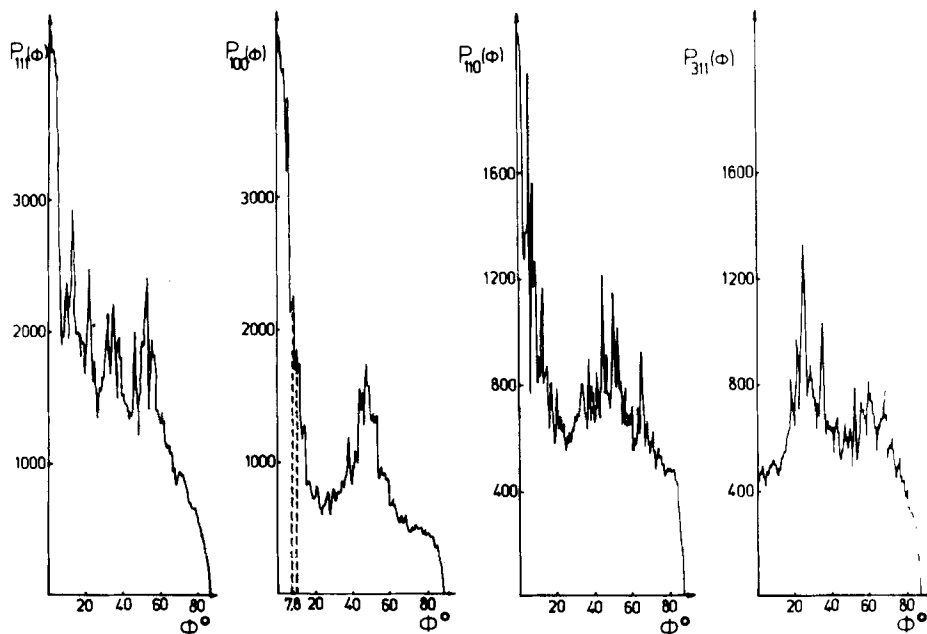


Fig. 4. Pole figures  $\{111\}$ ,  $\{100\}$ ,  $\{110\}$  and  $\{311\}$ . The texture components of the recrystallized texture are observed. The dotted line on angle  $\phi = 7.8^\circ$  (see  $P_{100}(\phi)$ ) marks the region where crystallites of component  $\langle 100 \rangle$  reflect, reflecting also the Debye ring 400.

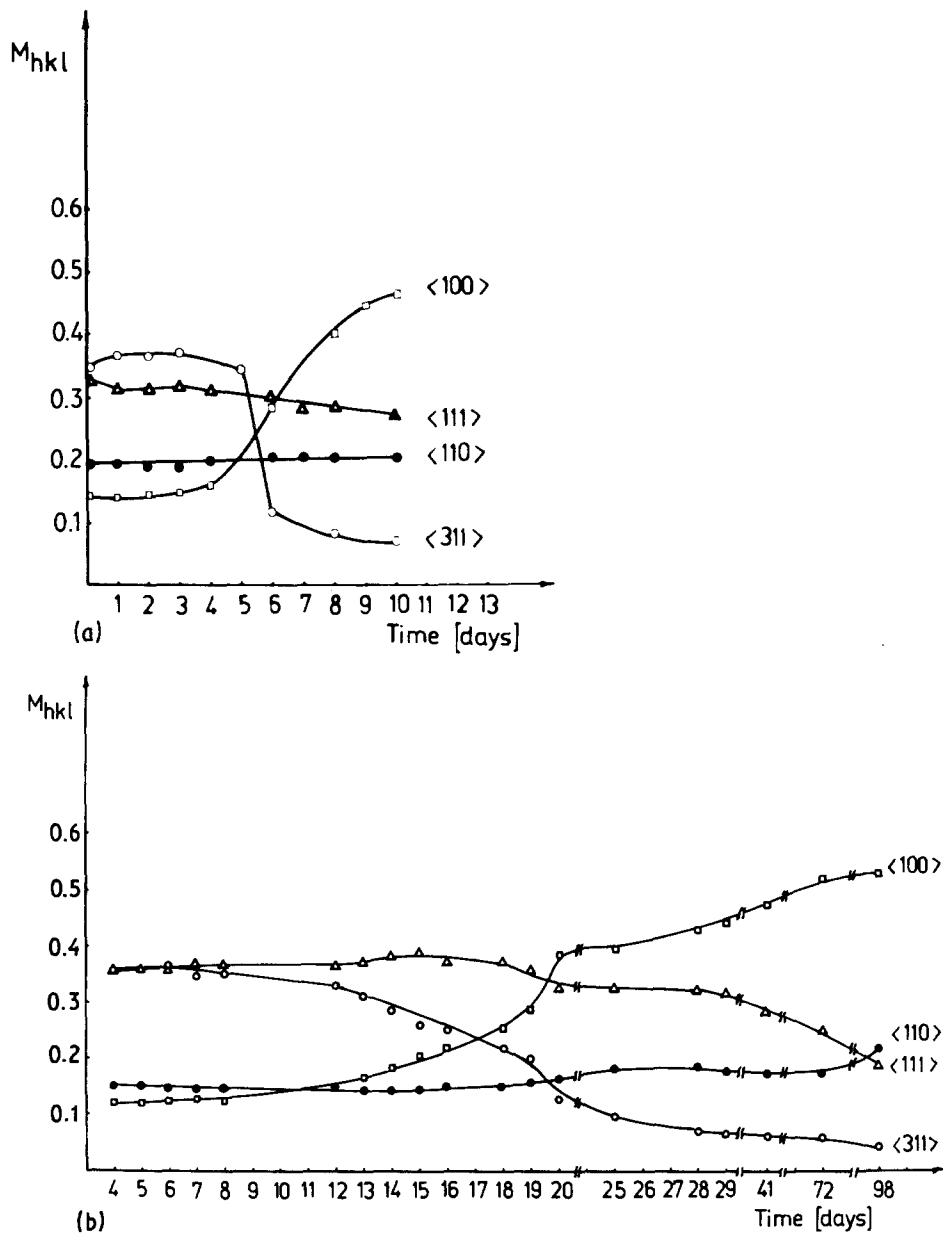


Fig. 5. Change of volume fractions  $M_{hkl}$  of texture components  $\langle 111 \rangle$ ,  $\langle 100 \rangle$ ,  $\langle 110 \rangle$  and  $\langle 311 \rangle$  with time. (a) Sample with rapidly falling microhardness (number 162). (b) Sample with slowly falling microhardness (number 163).

Scherrer camera, the appearance of recrystallization texture component  $\langle 100 \rangle$  becomes evident (Fig. 2), and a rough idea of the texture changes is gained from the qualitative investigations. However, fuller information on the structural changes occurring in the sample is not obtained. An estimation of the latter can be made if the change in the volume fractions  $M_{hkl}$

of the ideal positions  $\langle hkl \rangle$  is followed in time. This change in  $M_{hkl}$  is a quantitative characteristic of the orientation changes proceeding with time. The transformation changes presented in Fig. 5a, b for both samples (numbers 162 and 163) show that the recrystallization processes are essentially similar. An invariable phenomenon in both cases is that  $M_{311}$  and  $M_{111}$  decrease,

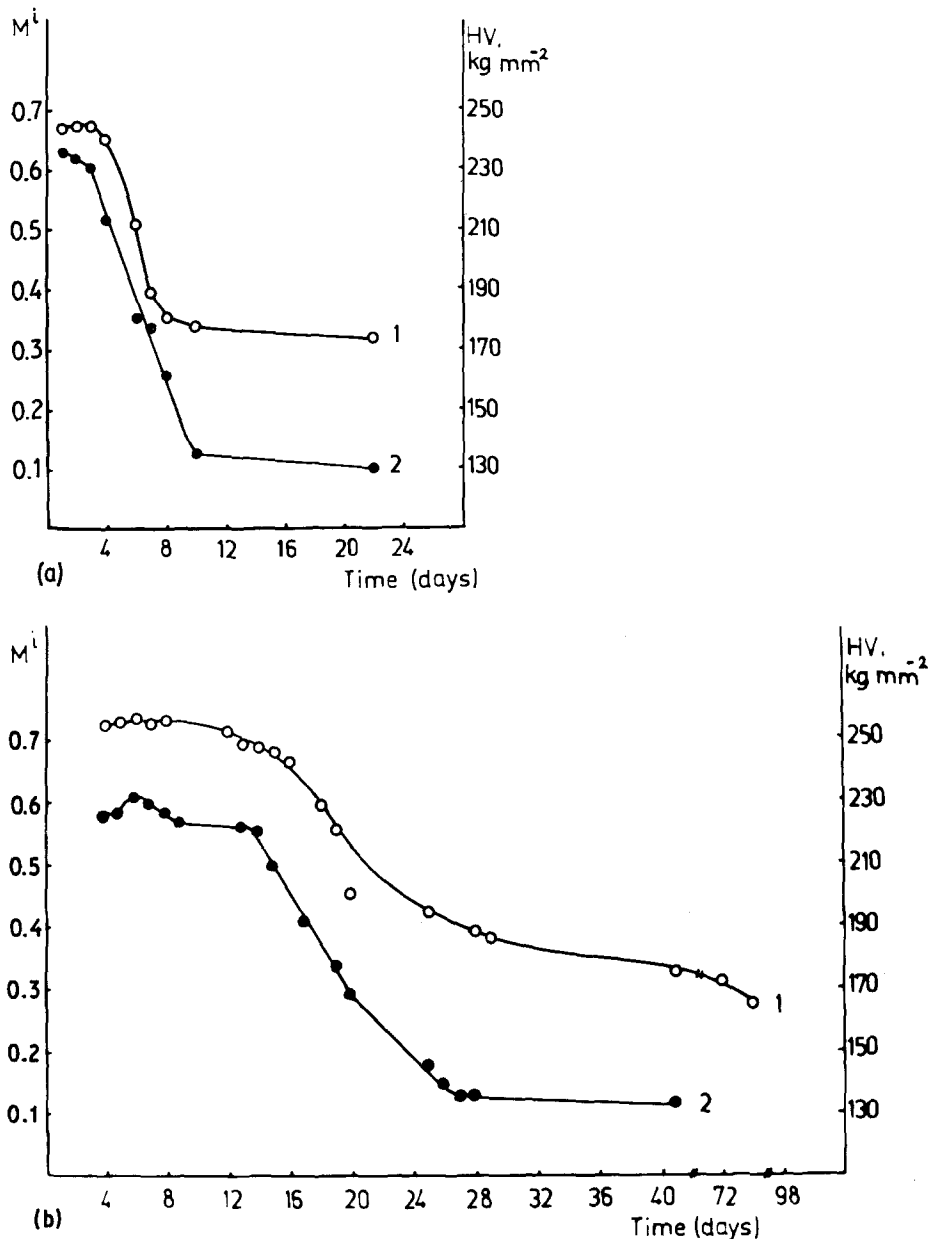


Fig. 6. Change in the sum of volume fractions  $M^i$  (curve 1) of decreasing components  $\langle 311 \rangle$ ,  $\langle 111 \rangle$  and microhardness HV (curve 2) with time. (a) Sample with rapidly falling microhardness (number 162). (b) Sample with slowly falling microhardness (number 163).

while  $M_{100}$  and  $M_{110}$  increase. The rates of the orientation changes are different. For sample number 162 a noticeable change in  $M_{hkl}$  was observed after the second or third day, the process being completed by about the tenth day. In sample number 163 the changes started after the tenth day and continued to about the 100th day.

The dependence of the sum of the volume fractions  $M^i$  of decreasing texture components with time for both samples is presented in Fig. 6a, b.

$$M^i = M_{311}^i + M_{111}^i \quad (4)$$

where  $i$  is the day when the measurement was made, i.e. 0, 1, 2, 3 and so on. In both cases the

decrease in  $M^i$  with time is accompanied by a similar course of the curves of sample microhardness (the microhardness data are taken from [17]). The contribution of the  $\langle 311 \rangle$  and  $\langle 111 \rangle$  components with their volume fractions  $M_{311}$  and  $M_{111}$  to the microhardness of the copper coatings is unambiguous. However, the microdeformations and the small apparent crystallite sizes are also responsible for the high microhardness. Moreover, it should be noted

that  $\langle 311 \rangle$  and  $\langle 111 \rangle$  components are built of crystallites with considerably deformed lattices, while the crystallites of the newly appearing components  $\langle 100 \rangle$  have quite small microdeformations of the crystal lattice.

5.4. *Texture transformations during primary recrystallization*

It was already established that during primary

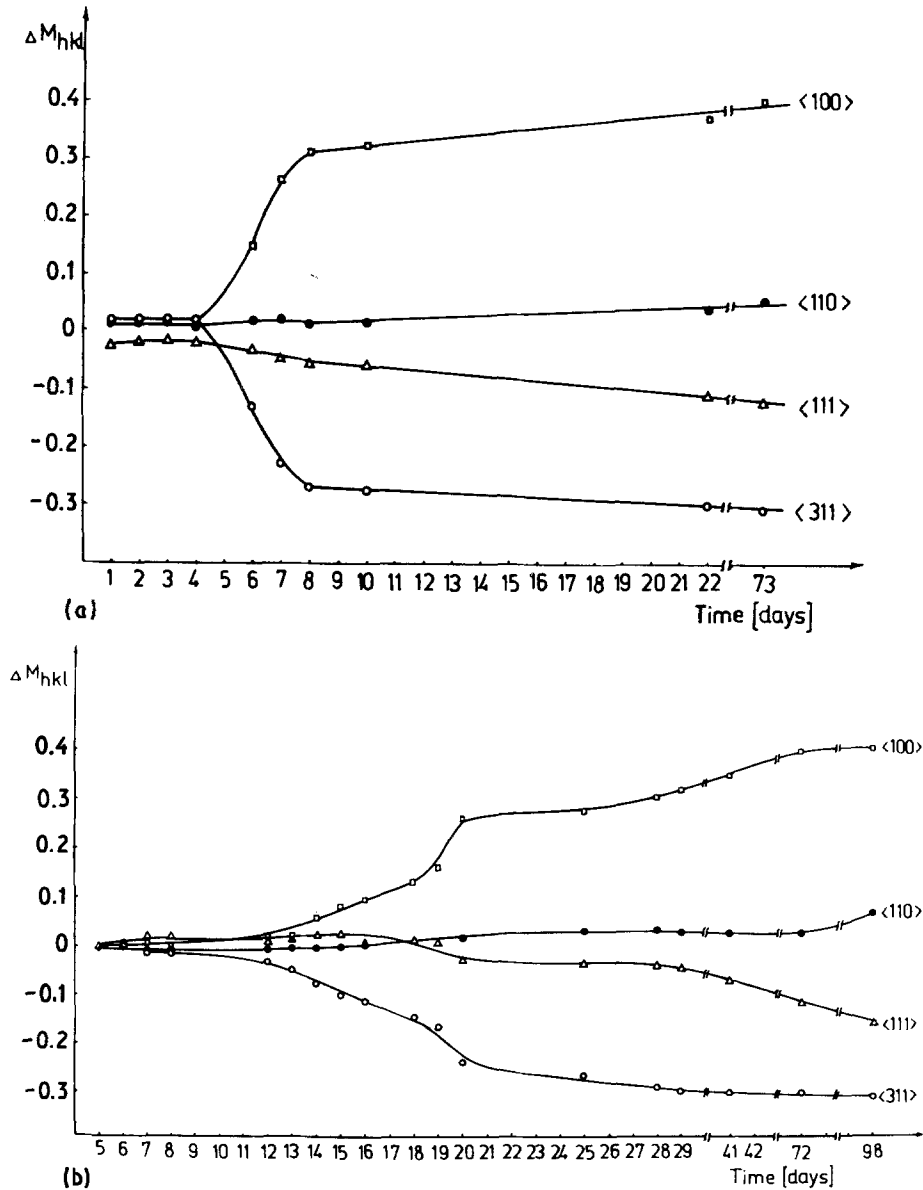


Fig. 7. Orientation relationships during recrystallization process: absolute change of the volume fractions  $M_{hkl}$  of texture components  $\langle 111 \rangle$ ,  $\langle 100 \rangle$ ,  $\langle 110 \rangle$ , and  $\langle 311 \rangle$  depending on time. (a) Sample with rapidly falling microhardness (number 162). (b) Sample with slowly falling microhardness (number 163).

recrystallization some of the growth texture components disappear and new components of the recrystallization texture appear. A study of the texture transformations during recrystallization could provide more complete information for the orientation relationship observed. An estimation of the texture transformations, i.e. the transition of one orientation into another, could be made from the absolute change in the volume fractions,  $\Delta M_{hkl}^i$ , of the respective components

$$\Delta M_{hkl}^i = M_{hkl}^i - M_{hkl}^0 \quad (5)$$

Fig. 7a, b presents these dependencies for sample numbers 162 and 163, respectively. It is evident that as a result of recrystallization, the crystallites of the  $\langle 311 \rangle$  growth texture component obtain a new orientation  $\langle 100 \rangle$ . At the same time, the volume fraction of the  $\langle 110 \rangle$  component also increases. This increase corresponds approximately to the decrease in the  $\langle 111 \rangle$  component. This supports the assumption that deformed crystallites with  $\langle 111 \rangle$  orientation recrystallize into grains with  $\langle 110 \rangle$  orientation.

It should be noted that the limited number of directions measured is a shortcoming of the experiment. It is limited by the wavelength of X-ray radiation used — the longer the wavelength, the smaller number of directions which could be measured. The error due to the small number of directions measured would influence the gradient of the curves, but would not change the direction of their course. Moreover, it must be noted that the orientations  $\langle 100 \rangle$ ,  $\langle 110 \rangle$ , and  $\langle 311 \rangle$  were reasonably chosen. It is evident from the pole figures (Figs 3, 4) that orientation changes do occur in these directions. Thus, regardless of the fact that the results for the volume fractions of the ideal positions are semi-quantitative, they are sufficient for the conclusions made.

## Conclusion

X-ray investigations *in situ* were carried out to study the recrystallization process in electro-deposited bright copper coatings at room tem-

perature. The growth texture is smeared out and has three components, i.e.  $\langle 311 \rangle$ ,  $\langle 111 \rangle$  and  $\langle 110 \rangle$ . The components of the recrystallization texture are  $\langle 100 \rangle$ ,  $\langle 110 \rangle$  and  $\langle 111 \rangle$ .

It is established that one of the factors influencing the microhardness is the orientation distribution of crystallites. The presence of  $\langle 311 \rangle$  and  $\langle 111 \rangle$  components favours high microhardness, while the recrystallization component  $\langle 100 \rangle$  contributes to the decrease in microhardness.

Semi-quantitative investigations of the orientation transformations between the growth texture and the recrystallization texture were carried out. It was found that the main texture component  $\langle 311 \rangle$  of the growth texture disappears and the recrystallization component  $\langle 100 \rangle$  appears. The assumption is made that part of the  $\langle 111 \rangle$  growth texture component is transformed into the  $\langle 110 \rangle$  component of the recrystallization texture.

## References

- [1] J. E. Burke and D. Turnbull, in 'Progress in Metal Physics', Vol. 3 (edited by B. Chalmers), Pergamon Press, London (1952) p. 220.
- [2] R. W. Cahn (ed), 'Physical Metallurgy', North-Holland Publishing Co., Amsterdam, 1965.
- [3] M. Cook and T. L. Richards, *J. Inst. Met.* **70** (1944) 159.
- [4] H. D. Megaw and A. R. Stokes, *ibid.* **71** (1945) 6.
- [5] J. S. Bowles and W. Boas, *ibid.* **66** (1940) 1.
- [6] C. S. Barrett, *Trans. Amer. Inst. Min. (Met.) Eng.* **137** (1940) 128.
- [7] M. L. Kornberg and F. H. Wilson, *ibid.* **185** (1949) 501.
- [8] P. A. Beck, P. R. Sperry and H. Hu, *J. Appl. Phys.* **21** (1950) 420.
- [9] P. A. Beck, *Acta Met.* **1** (1953) 230.
- [10] A. Merlini and P. A. Beck, *ibid.* **1** (1953) 598.
- [11] B. Liebmann, K. Luecke and G. Masing, *Z. Metallkde* **47** (1956) 57.
- [12] K. Luecke, *Can. Met. Quat.* **13** (1964) 261.
- [13] H. Hu, 'Textures of Materials' Vol. II, edited by G. Gottstein and K. Luecke, Springer-Verlag, Berlin, Heidelberg, New York (1978) 3.
- [14] K. Virnich, G. Kuehlhoff, K. Luecke and J. Pospiech, 'Textures of Materials', Vol. I, edited by G. Gottstein and K. Luecke, Springer-Verlag, Berlin, Heidelberg, New York (1978) 475.
- [15] I. Tomov and H. J. Bunge, *Texture Cryst. Sol.* **3** (1979) 73.
- [16] G. B. Harris, *Phil. Mag.* **43** (1952) 113.
- [17] D. Stoychev, I. Tomov and I. Vitanova, *J. Appl. Electrochem.* **15** (1985) 879.